Time-dependent loads on tunnel final linings

P. Yiouta-Mitra, A.I. Sofianos & S. Gekas
School of Mining Engineering, National Technical University of Athens, Greece

ABSTRACT: An analysis concerning the influence of time-dependent loads on the final lining is carried out using the finite element method. The loading induced by a drop in the bearing capacity of temporary support system and changes in the behaviour of geomaterials caused by swelling or creep phenomena is investigated and quantified. Two-dimensional plane strain models are employed for four Mohr-Coulomb types of geomaterials representative of characteristic RMR categories with deep circular openings under hydrostatic pressure.

1 SCOPE

The final lining of a tunnel is generally constructed after the temporary support system has reached conditions of equilibrium, the purpose of strongly reinforced final linings thus questioned. It is generally accepted that the final lining provides for increased safety as to the project lifetime and considers a number of load types of permanent, variable and accidental nature, such as, hydrostatic pressure, seismic forces, temperature changes. In addition, the final lining may be required to withstand loads resulting from deterioration of the preliminary support system, long term deformation of geomass and physical-chemical alterations of the rock/soil itself.

Within this framework, an analysis concerning the influence of the above time-dependent loads of the final lining is carried out using the finite element method aiming to quantify the induced loading.

1.1 Swelling

The phenomenon of swelling concerns time dependent strains that are due to a combination of physico-chemical activity related to water and stress regime. Under unconstrained conditions an immense increase in volume takes place. In regions where expansion is constrained by structural elements such as tunnel linings, significant compression states are likely to develop.

Grob (1972) provided the mathematical expression of the swelling rule and Einstein et al. (1972) assumed that the swelling rock behaves as an isotropic and linear elastic material and that results of one-dimensional oedometer tests can be extrapolated to three dimensions. An extensive coverage of methods and models can be found in ISRM, 1994. In the current research the numerical approach combined with the three-dimensional extension shall be used.

1.2 Creep

In some types of ground such as sheared or faulted rock masses containing mylonite or clay gouge, creep has been cited as the prime mechanism causing ground squeezing along with high stress field and extensive rockmass failure. Due to the time-dependent increase in ground movement and support load, such pressure on tunnel supports may increase for months or years after the completion of the excavation.

Creep behavior of geomaterials is commonly described by either rheological or empirical models. The former models that are commonly used only give a simple approximation of strain-stress time relationship of ground. The empirical models are usually expressed in simple mathematical forms with a small number of parameters and have been successfully used to describe observed creep behavior of soil and rock. The commonly used empirical creep models are the power law, the exponential law and the hyperbolic law (Phienwej et al., 2007).

1.3 Loss of temporary support

Temporary support measures may be considered to continue to be partly functional during the lifetime of a tunnel project. However, it is not unusual to ignore them during the final lining design due to gradual loss of bearing capacity, erosion of metal parts, shotcrete creep, inferior quality control.

Quantification of the amount of loading that is actually transferred to the final lining due to the temporary support loss is hereby performed.

2 NUMERICAL ANALYSES

The numerical code SOFISTIK was employed to perform the analyses. Two-dimensional plane strain models of Mohr-Coulomb geomaterial with deep

Table 1. Geomaterials and their mechanical properties.

Geomaterial Parameter	1	2	3	4
RMR	II–III	III–IV	I–II	II–III
v	0.35	0.3	0.3	0.3
E_m (MPa)	410	780	1648	559
φ (°)	27	24	35.1	31
c (kPa)	351	270	524	463
σ_t (kPa)	10	5	13	31

Table 2. Bearing capacity usage of temporary support measures.

Geomaterial	Rockbolts	Steelsets	Shotcrete
1	58.44%	64.34%	89.84%
2	29.44%	47.54%	59.61%
3	58.38%	92.14%	87.91%

Table 3. Pressure on the final lining caused by temporary support loss. Expressed as percentage of initial overburden load ($p^{final\ lining}/p_0$ %).

RMR	II–III	III–IV	I–II
p_i/p_0 @ tunnel face	20%	13%	42%
p_{ts}/p_0 @ 1 m from tunnel face	19.9%	13.1%	26.2%
Failed support measure			
Shotcrete	15.80%	11.50%	19.60%
Steelsets	0.90%	0.70%	1.20%
Rock Bolts	0.90%	0.10%	0.60%
All temporary support	20.20%	13.50%	21.70%

circular openings under hydrostatic pressure were first validated against the analytical solution of the convergence-confinement method (Panet, 1995).

Four types of geomaterials representative of characteristic RMR categories as depicted in Table 1 were then tested. Parameter selection was based on actual observations of shales, schists and marls.

All loads are presented in the form of p/p_0 where p_0 is the initial stress field at the depth of 20 tunnel diameters, which was held constant throughout the analyses.

Common starting point of all analyses is the load case where equilibrium between temporary support and rockmass pressure is reached, at 1m distance from the tunnel face. The entire construction procedure was therefore modeled beginning from the initial undisturbed conditions.

2.1 Temporary support loss

The temporary support system was common for all geomaterials in that it consisted of rockbolts Φ25 at 1.3 m in plane spacing, shotcrete C30/37 and C40/50 of varying thickness and steelsets HEB140 and an assumed excavation step of 1 m. It is important to note the numerical code limitation of support elements to elastic behavior, which has caused an apparent overdesign of temporary support measures, as can be seen in Table 2. Three dimensional temporary support installation was simulated in two stages, one for deconfinement at the tunnel face where rockbolts and 5 cm shotcrete were installed and the second at 1m distance from the tunnel face, where steelsets and total thickness of shotcrete were installed and equilibrium reached.

Table 3 contains the condensed results of the analyses for Rockmass types 1, 2 and 3. Firtsly, it can be seen that failure of shotcrete appears to be the most detrimental for the final lining loading. This is due to the fact that the other temporary support measures each contribute less than 10% of the required support pressure during construction. This depends on the construction sequence and the rockmass behaviour. Secondly, in the case of weaker rockmasses, all rockmass pressure at the tunnel face is transmitted to the temporary support and then to the final lining when temporary support fails. In the case of better ground conditions however, temporary support only contributes to the self-supporting capabilities of the ground and the subsequent loading of the final lining during failure is even less.

2.2 Swelling analyses

Modeling of swelling with the SOFISTIK code is based on a three-dimensional extension of the Grob (1972) constitutive law that relates the axial final state swelling strains to the present compression stress state, (Heidkamp et al., 2004). Introduction of a compressive limit stress σ_c provides equation (1) for calculation of swelling strains that have developed at the time $t = \infty$

$$
{}^{\infty}\varepsilon_{qi} = -k_q \begin{cases} 0 & , & \sigma_i \geq \sigma_{0i} \\ \log(\sigma_i/\sigma_0) & , & \sigma_{0i} > \sigma_i > \sigma_c \\ \log(\sigma_c/\sigma_0) & , & \sigma_i \leq \sigma_c \end{cases} \tag{1}
$$

where k_q = swelling modulus; σ_i = principal normal stress components; and σ_{0i} = normal components of initial equilibrium stress with respect to swelling.

Since this equation relates the final stationary state at $t = \infty$, it is then extended to the time evolution by defining the rate of swelling strains as

$$
\dot{\varepsilon}_q = \frac{\phi(\sigma, \varepsilon_q)}{\eta}; \phi(\sigma, \varepsilon_q) = {}^{\infty}\varepsilon_q(\sigma) - \varepsilon_q \tag{2}
$$

where the viscosity parameter η is the only scalar quantity. Integration of the swelling strain rate provides the evolution of swelling strains through time.

For the simple one-dimensional case an analytical solution is reached according to equation (3)

$$
e_q(t) = {}^{\infty}e_q(1 - e^{-t/\eta}) \tag{3}
$$

Table 4. Pressure p^{swel}/p_0 % on the final lining caused by swelling for geomaterial type 1.

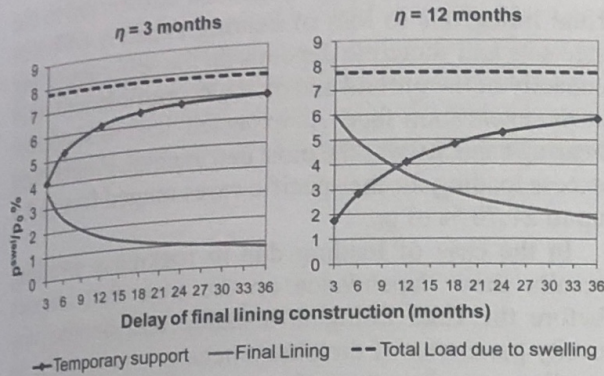| Delay in final lining construction (months)	Retardation time η (months)		
	$\eta = 3$	$\eta = 6$	$\eta = 12$
3	3.91	5.34	6.53
6	2.54	3.87	5.27
12	1.52	2.51	3.80
18	1.09	1.86	2.97
24	0.86	1.48	2.44
36	0.61	1.06	1.79

Figure 1. Effect of retardation time on swelling loading of final lining for geomaterial type 4.

In all performed analyses, parameter σ_{0i} was set equal to the initial stress field p_0 and $\sigma_c << p_i$ (pressure at the tunnel face) so as to ensure swelling throughout the entire construction process. The retardation time η was given 3 characteristic values: 3, 6 and 12 months while the entire phenomenon time was set at 50 years. Thus the condition $t/\eta \to \infty$ that ensures convergence was satisfied.

Geomaterials 1 and 4 were examined, giving slightly but not significantly different results. Total average loading due to swelling was 8.65% and 7.75% of p_0 for geomaterials 1 and 4 respectively.

The final lining loading was investigated by parameterizing the time of installation. It is expected that a late installation of the final lining will significantly reduce the loads due to swelling. However, retardation time was found to be an equally significant parameter as can be seen from Table 4 and Figure 1 that contain results for geomaterial types 1 and 4 respectively. Moreover, in the light of possible loss of the bearing capacity of the temporary support, the entirety of the loads may have to be considered for the final lining.

2.3 Creep analyses

The widely used viscoplastic formulation of the Perzyna (1966) model has been used for the simulation of creep phenomena. The main feature of this model is that the rate-independent yield function used for describing the viscoplastic strain can become larger than zero, effect known as 'overstress'. The rate of

the viscoplastic multiplier, also known as the consistency parameter, is explicitly defined via an overstress function (Heeres et al., 2000).

In the small-strain theory, the total strain rate in an elasto–viscoplastic material point may be additively decomposed into an elastic component and a viscoplastic component.

$$\dot{\varepsilon} = \dot{\varepsilon}^{el} + \dot{\varepsilon}^{vp} \tag{4}$$

Further, the viscoplastic strain rate evolves via a flow rule

$$\dot{\varepsilon}^{vp} = \dot{\lambda} m \tag{5}$$

where $\dot{\lambda} = $ consistency parameter specifying the magnitude and $m = m(\sigma, \Phi)$ determines the direction of $\dot{\varepsilon}^{vp}$; the second order tensor Φ reflects the evolution of the isotropic as well as the anisotropic internal variables.

The Perzyna theory defines the viscoplastic strain rate as

$$\dot{\varepsilon}^{vp} = \frac{\langle \phi(f) \rangle}{\eta} m; \langle \phi(\square) \rangle = \begin{cases} \phi(\square) & if \ \phi(\square) \geq 0 \\ 0 & if \ \phi(\square) < 0 \end{cases} \tag{6}$$

where $\eta = $ viscosity parameter, $\varphi = $ overstress function that depends on the rate-independent yield surface $f(\sigma, \Phi)$; and $m = \partial g/\partial \sigma$; $g = g(\sigma, \Phi)$ such that the rate effects are not affecting the direction of the viscoplastic flow.

Combining equations (5) and (6) the consistency parameter is explicitly expressed as

$$\dot{\lambda} = \frac{\langle \phi(f) \rangle}{\eta} \tag{7}$$

A widely used expression for the overstress function is

$$\phi(f) = (f/a)^N \tag{8}$$

where α is commonly chosen as the initial yield stress, and $N \geq 1$ is a calibration parameter.

Geomaterial type 1 was used as a basis for the creep analyses in combination with a sensitivity analysis of the rockmass elasticity modulus and the strength parameters c and φ. The viscosity parameter was set at 10^{12} kPa. The final lining loads were examined at three different assumed installation times. The creep phenomenon was given 100 years to fulfill its potential.

It can be seen from Figure 2 that 50% overestimation of the elasticity modulus more than doubles the pressure on final linings constructed a year after the temporary support. At 78% it is quintupled.

In Table 5 numerical values of creep loads on the final lining as compared to the total creep loads (temporary and final support) are provided. It is evident that the temporary support withstands most of the loads. This can be attributed to the use of elastic support elements whose bearing capacity was often not reached
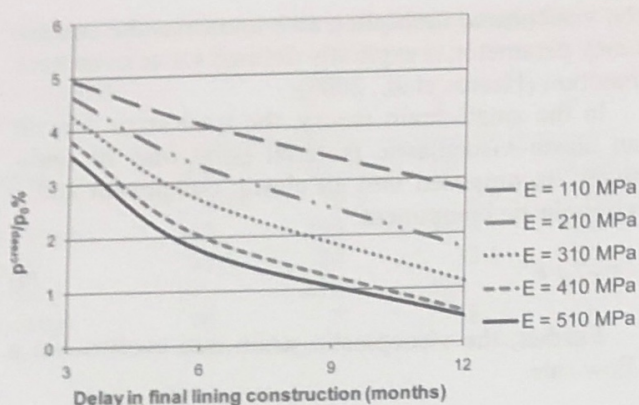
Figure 2. Effect of rockmass elasticity modulus on final lining pressure due to creep.

Table 5. Values of final lining and total loads due to creep (p^{creep}/p_0 %) for varying rockmass modulus of elasticity.

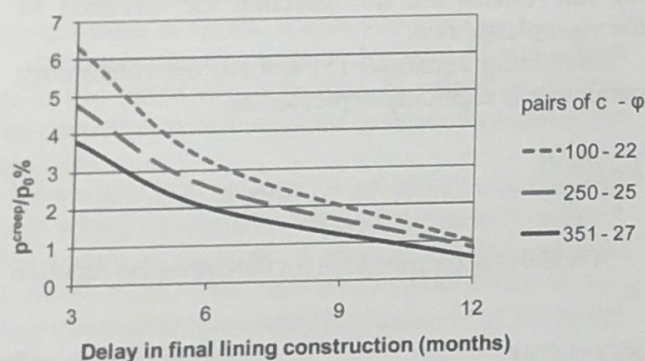| E (MPa)	Time of final lining construction (months)		
	3	6	12
510	3.53/15.03	1.75/14.97	0.49/14.93
410	3.81/15.15	2.01/15.13	0.57/15.12
310	4.25/15.37	2.66/15.39	1.11/15.42
210	4.62/15.78	3.30/15.86	1.74/15.94
110	4.93/16.76	4.07/16.87	2.80/17.03

Figure 3. Effect of strength parameters c (kPa) and φ (°) on final lining pressure due to creep.

Table 6. Values of final lining and total loads due to creep expressed as p^{creep}/p_0 % for variable strength parameters c and φ.

c(kPa)	φ(°)	Time of final lining construction (months)		
		3	6	12
351	27	3.81/15.15	2.01/15.13	0.57/15.12
250	25	4.76/18.80	2.55/18.78	0.82/18.77
100	22	6.30/24.91	3.23/24.83	0.96/24.78

during the temporary support – rockmass equilibrium load case.

Figure 3 and Table 6 contain creep load results that were acquired by changing the strength parameters of cohesion and angle of internal friction. In this case, the sensitivity is greater for earlier construction of the final lining. A more pronounced effect is also visible in the total loading due to creep. Although time of final lining construction still plays an important role in the magnitude of the final lining loading, the total creep load is more influenced by the variation in the strength parameters.

3 CONCLUSIONS

Parametric numerical analyses concerning the influence of time-dependent loads of the final lining have been carried out using the finite element method.

Results have shown that, the load transferred to the final lining due to loss of bearing capacity of bolts, steelsets and shotcrete depends on the self-supporting capacity of the ground and on the deconfinement ratio at the excavation face. As expected, loss of shotcrete bearing capacity was the most detrimental. Final lining excess loading for the specific cases ranged from 13.5 up to 21.70 % of p_0.

In the case of loading due to rockmass swelling results show dependance on the time that elapses before the final lining is installed and on the viscosity parameter of the phenomenon. Loading due to swelling was less than 1% up to 6.5% of the initial effective vertical stress p_0 for the specific cases that were investigated.

Loading due to creep showed dependency not only on time parameters but also on mechanical properties of the geomaterial and a range of 0.57%–6.3% of p_0 was determined for the final lining excess loading for the specific cases examined.

REFERENCES

Einstein H. H., Bischoff N. and Hofmann E., 1972. Behaviour of invert slabs in swelling shale, *Proc. Int. S. on Underground Openings*, Lucerne, Switzerland.

Grob H., 1972. Schwelldruck im Belchentunnel, *Proc. Int. S. On Underground Openings*, Lucerne, Switzerland.

Heeres O. M., Suiker A. S. J., de Borst R., 2002. A Comparison between the Perzyna Viscoplastic Model and the Consistency Viscoplastic Model, *European Journal of Mechanics A/Solids* 21, pp 1–12.

Heidkamp H., Katz C., 2004. The Swelling Phenomenon of Soils – Proposal of an Efficient Continuum Modelling Approach, *EUROCK 2004 & 53rd Geomechanics Colloquium*, Schubert (ed.), pp 1–6.

ISRM, 1994. Comments and Recommendations on Design and Analysis Procedures for Structures in Argillaceous Swelling Rock, Commission on Swelling Rock, *International Journal of Rock Mechanics, Mining Science & Geomechanics*, Abstr. Vol. 31, No 5, pp. 535–546.

Panet M., 1995. *Le calcul des tunnels par la methode convergence – confinement*, Paris: Presses de L'Ecole Nationale des Ponts et Chaussees.